Model calculations for ultrasonic plate - liquid - plate resonators: peak frequency shift by liquid density and velocity variations

1997 Meas. Sci. Technol. 8 643

(http://iopscience.iop.org/0957-0233/8/6/010)

Meas. Sci. Technol. **8** (1997) 643–647. Printed in the UK PII: S0957-0233(97)78146-3

Model calculations for ultrasonic plate–liquid–plate resonators: peak frequency shift by liquid density and velocity variations

Frieder Eggers

Max Planck-Institut für Biophysikalische Chemie, Abt 050, Postfach 2841, D37018 Göttingen, Germany

Received 26 September 1996, in final form 3 February 1997, accepted for publication 24 March 1997

Abstract. Ultrasonic resonators—consisting of the liquid sample, enclosed by two planar piezoelectric transducer plates—permit a direct and accurate determination of liquid sound velocities c_L at kilohertz and megahertz frequencies. Such plate–liquid–plate (PLP) resonators offer a resolution $\Delta c_L/c_L < 10^{-3}$, which is important for analytical work in chemistry, bio- and physico-chemistry and for some technical applications.

A simple one-dimensional resonator model is derived which permits calculation of the spectrum of the longitudinal (nonharmonic) eigenfrequencies f_n ($n = 1, 2, 3, 4\ldots$) as a function of liquid and resonator parameters. This model obtains the peak f_n shift by variation of liquid velocity c_L and density ρ_L as well for plane wave propagation; the effect from variations in ρ_L has been neglected in most ultrasonic studies so far.

Caused by a frequency-dependent phase shift for sound reflection at both liquid/transducer interfaces, the differential quotients $\mathrm{d}f_n/\mathrm{d}c_L$ and $\mathrm{d}f_n/\mathrm{d}\rho_L$ of the 'real' resonator deviate from those of an 'ideal' PLP resonator with perfect, 'hard' reflection (reflection factor $\equiv$1) and harmonic overtones nf_L (f_L is the liquid fundamental frequeny; one half liquid wavelength $\lambda_L/2$ equals transducer separation x).

The figures show typical acoustic impedance and admittance spectra, which are calculated for a model configuration; they illustrate features of the harmonic numbers in the liquid cavity and longitudinal mode counting. Equations are given for the dimensionless, normalized differential quotients $\mathrm{d}f_n/\mathrm{d}c_L \cdot c_L/f_n$ and $\mathrm{d}f_n/\mathrm{d}\rho_L \cdot \rho_L/f_n$. Plots demonstrate systematic aberrations from 'ideal' resonator behaviour, which can affect high-precision sound velocity measurements.

1. Introduction

Ultrasonic PLP resonators, consisting of two air-backed, planar piezoelectric transducers and the enclosed liquid sample (volume ~0.1–10 ml), are a valuable tool for the determination of liquid sound absorption and velocity in the 0.1 to 100 MHz range (Eggers 1967/68, 1992, 1994, Eggers and Funck 1973, Eggers *et al* 1994, Eggers and Kaatze 1996, Kaatze *et al* 1987, Labhardt and Schwarz 1976, Sarvazyan 1982, Sarvazyan and Chalikian 1991). Resonator eigenfrequencies f_n can be obtained with high resolution, particularly in low-loss liquids, by means of amplitude, phase, phase slope or group delay time $t_g = -\mathrm{d}\varphi/\mathrm{d}\omega$ (φ is the phase, ω the angular frequency) measurements. From a series of f_n values the liquid column fundamental frequency $f_L = c_L/2x$ and—with the liquid pathlength or transducer separation x known—the sound velocity c_L can be determined by nonlinear regression, which also yields the specific acoustic impedance ratio $z_L/z_T = (\rho_L c_L)/(\rho_T c_T)$ (ρ is the density) for longitudinal, plane wave propagation in the liquid (L) and the transducer medium (T; X-cut quartz or Y-cut lithium niobate in most devices).

If the sound beam diameter D exceeds the wavelength λ_L ($D > 50\lambda_L$), *one-dimensional, plane wave* equations describe the performance of such PLP resonators to a very good approximation (Eggers 1992). Piezoelectric coupling in the transducer material, given by the electromechanical coupling coefficient k_T (Kino 1987), affects the eigenfrequencies, including the overtones, of the transducer plates (Onoe *et al* 1963). The piezoelectric effect can be taken into account by introducing *effective* eigenfrequencies f_{Tm}, but it causes loading of the cavity due to electromechanical energy coupling, particularly at the transducer fundamental and overtones.

0957-0233/97/060643+05$19.50

For applications in ultrasonic *velocimetry* (Sarvazyan 1982, 1991) it is desirable to know the influence of liquid velocity c_L and density ρ_L and of their changes on the eigenfrequencies f_n ($n = 1, 2, 3, \ldots$) quantitatively. This dependence can be obtained from the derivatives $\mathrm{d}f_n/\mathrm{d}c_L$ and $\mathrm{d}f_n/\mathrm{d}\rho_L$ of a characteristic trigonometric equation $F(f_n,\ f_T,\ x,\ c_L,\ \rho_L,\ c_T,\ \rho_T) = 0$, which permits determination of the fundamental frequency of the liquid column f_L and of the f_n spectrum (Eggers 1967/68, 1992, Eggers and Richmann 1993).

2. Acoustic resonator eigenfrequencies—one-dimensional model

The characteristic acoustical *impedance* equations for PLP resonators relate f_n to the sample parameters c_L, ρ_L, f_L and to the corresponding piezotransducer parameters c_T, ρ_T and f_T (fundamental frequency; plate thickness equals $\lambda_T/2$). Usually the compressional waves in the liquid cavity undergo nearly 'hard' reflection due to the higher specific impedance $z_T > z_L$ of the transducers, except at the fundamental f_T and the overtones f_{Tm}, where the wave 'sees' the low backing (air!) impedance. Usually the region near f_T is not employed for velocity and absorption measurements, because enhanced electromechanical energy coupling in the transducers—stronger in $LiNbO_3$ than in quartz—decreases the cavity Q, in addition to liquid absorption. It is advisable to refer the nonharmonic f_n series of the PLP resonator and its harmonic numbers n to the harmonic spectrum nf_L of an 'ideal' resonator with perfect reflection ($r \equiv 1$). The harmonic number $n = 1, 2, 3, 4\ldots$ of such resonators is approximately the number of half-wavelengths $\lambda_L/2$ in the liquid standing wave field: $n \approx 2x/\lambda_L$. The impulse balance of the total vibrating system is established by the mass of the cavity vessel and frame plus the affixed transducers, this being large compared to the liquid mass.

In consequence of resonator symmetry, oscillational modes of the compound PLP system have either a particle velocity extremum and a pressure node (n odd) or a particle velocity node and a pressure extremum (n even) in the *centre plane* of the resonator. Therefore it is sufficient to consider one half of the resonator, consisting of *one* transducer and *half* of the liquid column (assumed to be lossless), terminated in the centre plane either by impedance zero (n odd) or by infinite impedance (n even). The acoustic impedance Z (per unit area) is the complex ratio of sound pressure to particle velocity at a point (or plane) in the sound field (Gooberman 1968). Resonance occurs for reactance compensation at the liquid–transducer interface or the equality and opposite sign for the imaginary parts of transducer impedance Z_T and liquid impedance Z_L (pathlength $x/2$), i.e. $\mathrm{Im}(Z_T) = -\mathrm{Im}(Z_L)$ (Eggers 1967/68). For a plane wave field:

$$Z_T = \mathrm{i}z_T \tan\left(\pi \frac{f_n}{f_T}\right) \tag{1}$$

$$Z_L = \left\langle \begin{matrix} + \\ - \end{matrix} \right\rangle \mathrm{i}z_L \left\langle \begin{matrix} \tan \\ \cot \end{matrix} \right\rangle \left(\frac{\pi}{2}\frac{f_n}{f_L}\right) \qquad \left\langle \begin{matrix} n & \text{odd} \\ n & \text{even} \end{matrix} \right\rangle . \qquad \begin{matrix} (2a) \\ (2b) \end{matrix}$$

It should be noted that the assignment of odd and even n in equations (2a) and (2b) is different from that in some earlier publications, apparently erroneous. Both equations can be combined in one equation, valid for odd and even n as well

$$Z_L = -\mathrm{i}z_L \cot\left[\frac{\pi}{2}\left(\frac{f_n}{f_L} - n\right)\right]. \tag{2c}$$

Equations (1) and (2c) lead to a characteristic equation $Z_T = -Z_L$, which determines the series of f_n for a one-dimensional plane wave PLP resonator

$$z_T \tan\left(\pi \frac{f_n}{f_T}\right) = z_L \cot\left[\frac{\pi}{2}\left(\frac{f_n}{f_L} - n\right)\right]. \tag{3}$$

For certain applications peak frequencies close to $f_T/2$, $3f_T/2$, $5f_T/2$ etc, with the transducer thickness being an odd multiple of $\lambda_T/4$, are of particular interest, because the low air backing impedance of the transducer is inverted by a 'quarter-wavelength-transformation', resulting in 'infinite' impedance behaviour and hard reflection between liquid and transducers.

Equations (1) and (2c) yield the corresponding acoustic *admittances*

$$A_T = -\frac{\mathrm{i}}{z_T} \cot\left(\pi \frac{f_n}{f_T}\right) \tag{4}$$

$$A_L = \frac{\mathrm{i}}{z_L} \tan\left[\frac{\pi}{2}\left(\frac{f_n}{f_L} - n\right)\right] \tag{5}$$

resulting in a characteristic equation, which is equivalent to equation (3)

$$\frac{1}{z_T} \cot\left(\pi \frac{f_n}{f_T}\right) = \frac{1}{z_L} \tan\left[\frac{\pi}{2}\left(\frac{f_n}{f_L} - n\right)\right]. \tag{6}$$

Here the cases $n = 1$ and $n = 2$ cover all odd and even longitudinal modes. The anharmonicity of the f_n spectrum in the frequency range 2–10 MHz is illustrated in figure 1 for *impedance* and in figure 2 for *admittance*, depicting the terms of equations (1) and (2c) and (4) and (5) respectively. The intersections of $-Z_L$ (conjugate complex) with Z_T and $-A_L$ (conjugate complex) with A_T determine the f_n spectrum. It is obvious that *impedance* relations are preferable at and near the odd transducer harmonics f_T, $3f_T$, $5f_T$ etc—the even harmonics of f_T are sonically inactive—while *admittance* is advantageous near $f_T/2$, $3f_T/2$, $5f_T/2$, etc. In figure 2 the intersections of $-A_L$ with the abscissa define the harmonics of f_L, i.e. the spectrum of an 'ideal' resonator with infinitely hard ($z_T = \infty$) reflectors. It appears reasonable to refer the resonances of a 'real' resonator to the nearby harmonics nf_n. In order to illustrate mode numbering around f_T, figure 3 shows an expanded plot of $-A_L$ and A_T between 4 and 6 MHz for water and quartz transducers, now with $f_T = 5100$ kHz assumed for clarity. It reveals, that the $-A_L$ branch ($n = 10$) has *two* intersections with A_T; the same is true for the neighbouring branch ($n = 11$). In this case four subsequent peaks f_{10-}($\sim$4793 kHz), f_{11-}($\sim$5001 kHz), f_{10+}($\sim$5208 kHz) and f_{11+}($\sim$5582 kHz) are observed. Peak f_{11-} originates from a 'soft' reflection with low Z_T at transducer $\lambda_T/2$ resonance. On the other hand, if

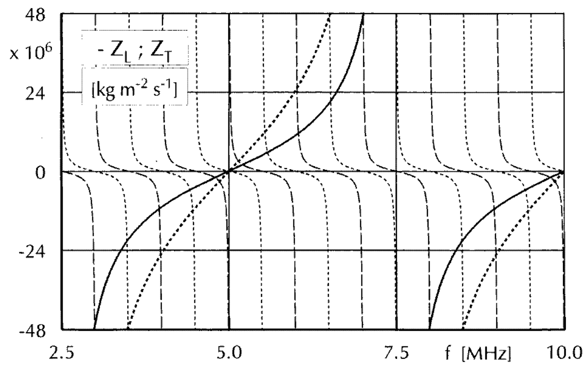

Figure 1. Calculated acoustic impedance Z (per unit area; imaginary part) versus frequency f: Z_T for X-cut quartz (—— z_T^{quartz} = 15 × 10^6 kg m^{-2} s^{-1}) and for Y-cut lithium niobate (··· $z_T^{niobate}$ = 34 × 10^6 kg m^{-2} s^{-1}) transducers; f_T = 5000 kHz. $-Z_L$ for odd (- - - -) and even (— — —) modes in water at pathlength $x/2$; c_L = 1.5 km s^{-1}, ρ_L = 10^3 kg m^{-3}, x = 1.5 mm, f_L = 500 kHz. Intersections between Z_T and $-Z_L$ branches determine the resonant frequencies f_n.

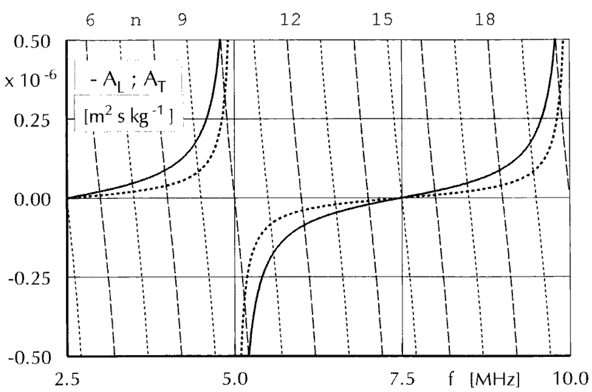

Figure 2. Calculated acoustic admittance A (per unit area, imaginary part): A_T (quartz and lithium niobate) and $-A_L$ for odd and even modes in water. Curve types and parameters as in figure 1. Intersections of A_T and $-A_{L,n}$ branches determine f_n values. Harmonic numbers n, given at the top of the plot are characterized by abscissa crossing points $A_{L,n}$ = 0 and refer f_n series to harmonic spectrum nf_L of an 'ideal' resonator with 'hard' reflection ($z_T = \infty$).

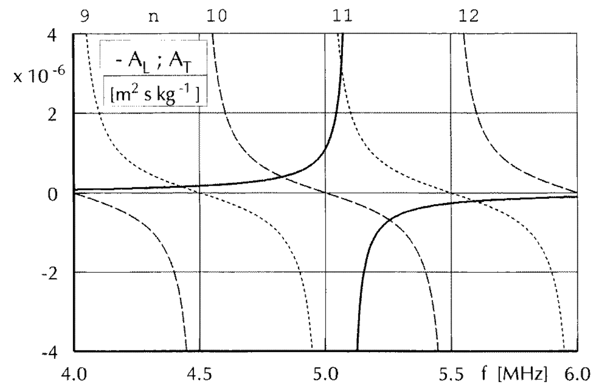

Figure 3. Calculated acoustic admittance (per unit area, imaginary part): A_T (quartz; f_T = 5100 kHz) and $-A_L$ for odd and even longitudinal modes in water. Curve types and other parameters as in figure 1. Harmonic numbers n shown at the top of the plot.

$f_T < 10 f_L$ is assumed, the sequence around f_T changes to f_{9-}, f_{10-}, f_{9+}, f_{10+}. Model parameters used are listed in the captions. Liquid loss is always neglected and one-dimensional, plane wave propagation is assumed.

From the implicit admittance equation

$$F = \frac{1}{\rho_T c_T} \cot\left(\pi \frac{f_n}{f_T}\right) - \frac{1}{\rho_L c_L} \tan\left[\frac{\pi}{2}\left(\frac{f_n}{c_L/2x} - n\right)\right] = 0 \tag{7}$$

the differential quotients $\mathrm{d}f_n/\mathrm{d}\rho_L$ and $\mathrm{d}f_n/\mathrm{d}c_L$ are obtained, using common mathematical rules for the differentiation of implicit functions (e.g. Korn and Korn 1968)

$$\frac{\mathrm{d}f_n}{\mathrm{d}c_L} = -\frac{\partial F}{\partial c_L}\bigg/\frac{\partial F}{\partial f_n} \qquad \frac{\mathrm{d}f_n}{\mathrm{d}\rho_L} = -\frac{\partial F}{\partial \rho_L}\bigg/\frac{\partial F}{\partial f_n} \qquad (8),\ (9)$$

leading—after some manipulation—to

$$\begin{aligned}\frac{\mathrm{d}f_n}{\mathrm{d}c_L} = \frac{f_n}{c_L}&\left\{1 + \frac{1}{\pi}\frac{f_L}{f_n}\sin\left[\pi\left(\frac{f_n}{f_L} - n\right)\right]\right\}\\ &\times\left[\!\left[1 + 2\frac{z_L}{z_T}\frac{f_L}{f_T}\left\{\cos\left[\frac{\pi}{2}\left(\frac{f_n}{f_L} - n\right)\right]\right\}^2\right.\right.\\ &\left.\left.\times\left\{\sin\left[\pi\frac{f_n}{f_T}\right]\right\}^{-2}\right]\!\right]^{-1}\end{aligned} \tag{10}$$

the second factor being dimensionless, and to

$$\begin{aligned}\frac{\mathrm{d}f_n}{\mathrm{d}\rho_L} = \frac{f_n}{\rho_L}&\left\{\frac{1}{\pi}\sin\left[\pi\left(\frac{f_n}{f_L} - n\right)\right]\right\}\\ &\times\left[\!\left[\frac{f_n}{f_L} + 2\frac{z_L}{z_T}\frac{f_n}{f_T}\left\{\cos\left[\frac{\pi}{2}\left(\frac{f_n}{f_L} - n\right)\right]\right\}^2\right.\right.\\ &\left.\left.\times\left\{\sin\left[\pi\frac{f_n}{f_T}\right]\right\}^{-2}\right]\!\right]^{-1}.\end{aligned} \tag{11}$$

For an 'ideal' resonator ($r \equiv 1$) the spectrum $f_n^{ideal} = nf_L = nc_L/2x$ is harmonic; in this case is $\mathrm{d}f_n^{ideal}/\mathrm{d}c_L = n/2x = f_n/c_L$, a commonly used approximation for equation (10); on the other hand $\mathrm{d}f_n^{ideal}/\mathrm{d}\rho_L \equiv 0$ is in clear contrast to equation (11).

For a plot of equations (10) and (11) numerical f_n values ($n = 4 \ldots 20$) have been calculated directly from equation (7). Another proven way to obtain numerical values of the f_n series is by iteration, starting from $f_n^{\langle 0\rangle} = nf_L$ and using the relation, which results from equation (7)

$$f_n^{\langle m+1\rangle} = f_L\left\{n + \frac{2}{\pi}\tan^{-1}\left[\frac{z_L}{z_T}\cot\left(\pi\frac{f_n^{\langle m\rangle}}{f_T}\right)\right]\right\}. \tag{12}$$

However, in pursuing this way convergence might fail near f_T and its harmonics.

Figure 4 shows a plot of the dimensionless $(\mathrm{d}f_n/\mathrm{d}c_L) \times (c_L/f_n)$, equivalent to $\mathrm{d}(\ln f_n)/\mathrm{d}(\ln c_L)$, for the calculated f_n values between 2 and 10 MHz. The f_n points ($n = 4 \ldots 20$) represent even and odd acoustic modes in the water-filled cavity ($f_L = 500$ kHz), enclosed by transducers from X-cut quartz (specific impedance value $z_{X-quartz} \approx 15 \times 10^6$ kg m^{-2} s^{-1}) and Y-cut $LiNbO_3$ ($z_{LiNbO_3} \approx 34 \times 10^6$ kg m^{-2} s^{-1}). In a similar way the differential

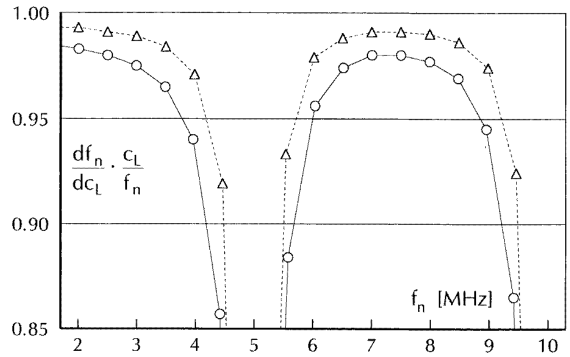

Figure 4. Calculated normalized differential quotient $(\mathrm{d}f_n/\mathrm{d}c_L) \times (c_L/f_n) = \mathrm{d}\ln f_n/\mathrm{d}\ln c_L$ for odd and even mode resonant frequencies f_n. Transducers f_T = 5001 kHz: ○, quartz; △, lithium niobate. Other parameters as in figure 1.

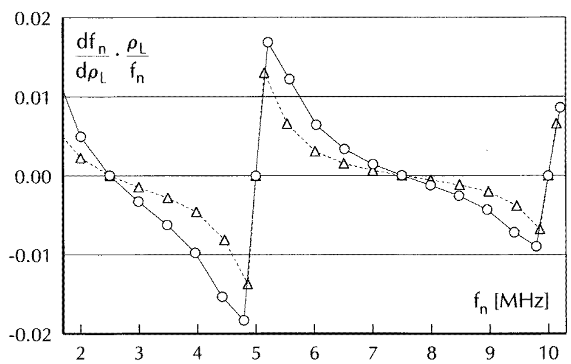

Figure 5. Calculated normalized differential quotient $(\mathrm{d}f_n/\mathrm{d}\rho_L) \times (\rho_L/f_n) = \mathrm{d}\ln f_n/\mathrm{d}\ln \rho_L$ for odd and even mode resonant frequencies f_n. Transducers f_T = 5001 kHz: ○, quartz; △, lithium niobate. Other parameters as in figure 1.

quotient $\mathrm{d}f_n/\mathrm{d}\rho_L \times \rho_L/f_n = \mathrm{d}(\ln f_n)/\mathrm{d}(\ln \rho_L)$ versus f_n is displayed in figure 5 for quartz and for $LiNbO_3$ transducers. Peak f_n shifts from *density* variation increase near f_T, pointing at the possibility for liquid density measurements with ultrasonic resonators. Equivalents of equations (10) and (11) could also be derived from *impedance* relations, particularly near f_T and its overtones, but are not given here because of space limitations.

Equations have been solved numerically with the software MATHCAD® 6.0 SE from MathSoft (command 'root') or with MAPLE® V3 ('fsolve'). For initial plotting and for symbolic differentiation of functions MATHCAD® 6.0 SE and its incorporated MAPLE® components have been used; controls have been made with the numerical differentiation algorithm in MATHCAD® 6.0 SE, yielding identical results. All figures have been obtained with AXUM® (version 4.1) from MathSoft.

3. Discussion and conclusions

The plots demonstrate that liquid density as well as velocity shifts cause typical resonant peak shifts in ultrasonic PLP resonators, differing from 'ideal' resonator behaviour and depending on frequency and on transducer parameters. At first sight it might be surprising, that even at transducer '$\lambda_T/4$ frequencies' $f_T/2$, $3f_T/2$, $5f_T/2\ldots$, the maximum of $\mathrm{d}f_n/\mathrm{d}c_L \times c_L/f_n$ is slightly below 1. This is quantified by an approximation of equation (10) at those frequencies

$$\frac{\mathrm{d}f_n}{\mathrm{d}c_L}\,\frac{c_L}{f_n} \approx 1 - 2\frac{z_L}{z_T}\,\frac{f_L}{f_T} \tag{13}$$

yielding 0.98 at 7.5 MHz for a water-filled quartz resonator ($z_L/z_T = 0.1$; $f_L = 0.5$ MHz; $f_T = 5$ MHz). This is reasonable because the liquid velocity c_L affects both f_L and Z_L, shifting nf_L and the reflection phase in an opposing way. On the other hand the maximum value of $\mathrm{d}f_n/\mathrm{d}c_L \times c_L/f_n$ becomes closer to 1 for resonators with increased pathlength x and in consequence lower f_L, because fewer reflections will then occur in the cavity. Please note that near f_T and $2f_T$ the values $\mathrm{d}f_n/\mathrm{d}c_L \times c_L/f_n$ fall below 0.6 and are not shown in figure 4 with its expanded ordinate scale.

The effect from density variations is minimized near the '$\lambda_T/4$ frequencies' $f_T/2$, $3f_T/2$, $5f_T/2$, etc, but is *zero* only *exactly* at those. Figure 5 shows that the density influence increases in regions below and above f_T and its overtones; here liquid density can be determined by ultrasonic measurements via the specific impedance ratio z_L/z_T. High-resolution measurements of velocity ($|\delta f_n|/f < 10^{-6}$), aiming at adiabatic compressibility values (Sarvazyan 1991), have to take density into account, since *both* liquid velocity and density affect the f_n spectrum.

A reliable, proven way for velocity evaluation, including density effects, is to measure a series of 3 to 11 (and possibly more) subsequent f_n values around the '$\lambda_T/4$ frequencies' $f_T/2$, $3f_T/2$, or $5f_T/2$. Nonlinear regression, applying equation (6) and a LEVENBERG–MARQUARDT algorithm (command 'minerr' in MATHCAD®), helps to identify the harmonic numbers n and obtains both f_L and z_L/z_T. Assuming plane wave propagation at sufficiently high frequencies, an extra check of measured f_n values and n is to apply equation (6) again and calculate a series of individual liquid fundamental $f_{L,n}$ values:

$$f_{L,n} = f_n \left\{ n + \frac{2}{\pi}\tan^{-1}\left[\frac{z_L}{z_T}\cot\left(\pi\frac{f_n}{f_T}\right)\right]\right\}^{-1} \tag{14}$$

which should be constant and close (within a few Hz and less for 3 to 5 peaks) to the f_L value obtained by regression. This has been verified in many experiments near 7.5 and 12.5 MHz. For the evaluation of resonant peaks with accompanying spurious 'satellites' further precautions are advisable: a regression procedure should be preceeded by an algebraic separation of superposing acoustic modes and of eventual electromagnetic crosstalk (Eggers 1992). Peak frequencies can be 'pinned' by means of the: (a) amplitude maximum; (b) algebraic fit of sampled amplitude values of a total peak; (c) algebraic fit of sampled phase values of a total peak; (d) maximum of group delay time (phase slope); (e) algebraic fit of sampled group delay time values of a total peak. The method to be preferred depends on the available equipment. The evaluation of a total peak as in (b) or in (c) appears to be more accurate than the search for a rather 'flat' amplitude top. Methods (d) and (e) gain from the elimination of a base line phase shift caused by electrical connections, but require more sophisticated electronic equipment.

In general ultrasonic resonator measurements are affected by several sources of error. One has to realize the practical limits of accuracy, which are given primarily by sound field diffraction, by liquid absorption and, last but not least, by temperature fluctuations in the liquid cavity. For practical applications these model calculations should be seen in the frame of the total accuracy obtainable today for high-precision acoustic measurements in liquids.

Acknowledgments

Thanks go to Professor Leo De Maeyer for stimulating discussions and to Dr Udo Kaatze and Mr Kurt-Helmut Richmann for valuable advice.

References

Eggers F 1967/68 Eine Resonatormethode zur Bestimmung von Schallgeschwindigkeit und Dämpfung an geringen Flüssigkeitsmengen *Acustica* **19** 323–9

——1992 Ultrasonic velocity and attenuation measurements in liquids with resonators, extending the MHz frequency range *Acustica* **76** 231–40

——1994 Analysis of phase slope or group delay time in ultrasonic resonators and its application for liquid absorption and velocity measurements *Acustica* **80** 397–405

Eggers F and Funck Th 1973 Ultrasonic measurements with milliliter liquid samples in the 0.5–100 MHz range *Rev. Sci. Instrum.* **44** 969–77

Eggers F and Kaatze U 1996 Broad-band ultrasonic measurement techniques for liquids *Meas. Sci. Technol.* **7** 1–19

Eggers F, Kaatze U, Richmann K-H and Telgmann T 1994 New plano-concave ultrasonic resonator cells for absorption and velocity measurements in liquids below 1 MHz *Meas. Sci. Technol.* **6** 1131–8

Eggers F and Richmann K-H 1993 Ultrasonic absorption measurements in liquids above 100 MHz with continuous waves, employing algebraic crosstalk elimination *Acustica* **78** 27–35

Gooberman G L 1968 *Ultrasonics* (London: English University Press)

Kaatze U, Wehrmann B and Pottel R 1987 Acoustical absorption spectroscopy of liquids between 0.15 and 3000 MHz: I. High resolution ultrasonic resonator method *J. Phys. E: Sci. Instrum.* **20** 1025–30

Kino G S 1987 *Acoustic Waves: Devices, Imaging, and Analog Signal Processing* (Englewood Cliffs, NJ: Prentice-Hall)

Korn G A and Korn Th M 1968 *Mathematical Handbook for Scientists and Engineers* 2nd edn (New York: McGraw-Hill) p 100

Labhardt A and Schwarz G 1976 A high resolution and low volume ultrasonic resonator method for fast chemical relaxation measurements *Ber. Bunsenges.* **80** 83–92

Onoe M, Tiersten H F and Meitzler A H 1963 Shift in the location of of resonant frequencies caused by large electromechanical coupling in thickness-mode resonators *J. Acoust. Soc. Am.* **35** 36–42

Sarvazyan A P 1982 Development of methods of precise ultrasonic measurements in small volumes of liquids *Ultrasonics* **20** 151–4

——1991 Ultrasonic velocimetry of biological compounds *Ann. Rev. Biophys. Biophys. Chem.* **20** 321–42

Sarvazyan A P and Chalikian T V 1991 Theoretical analysis of ultrasonic interferometer for precise measurements at high pressures *Ultrasonics* **29** 119–24